Segregation and phase inversion of strongly and weakly fluctuating Brownian particle mixtures and a chain of such particle mixtures in spherical containers

Akinori Awazu

Department of Mathematical and Life Sciences, Hiroshima University, Kagami-yama 1-3-1, Higashi-Hiroshima 739-8526, Japan and Research Center for Mathematics on Chromatin Live Dynamics. Kagami-yama 1-3-1, Higashi-Hiroshima 739-8526, Japan

(Received 25 April 2014; revised manuscript received 21 August 2014; published 17 October 2014)

We investigate the segregation pattern formation of strongly and weakly fluctuating Brownian particle mixtures confined in a three-dimensional spherical container. We consider systems where the particle motion is restricted by the harmonic external trapping potential and the container edge wall. In such systems, two segregation patterns are observed. When the container radius is sufficiently large, more weakly fluctuating particles accumulate near the center of the container than strongly fluctuating particles. On the other hand, the distributions of the strongly and weakly fluctuating particles are inverted when the container radius is small. With no external trapping potentials, we find similar segregation and phase inversion if the particles construct a chain (heterofluctuating polymer) and are confined in a three-dimensional spherical container. We could apply these phenomena in the study of biopolymer behavior, such as chromosomes in the cell nucleus.

DOI: 10.1103/PhysRevE.90.042308 PACS number(s): 64.75.Xc, 87.15.Zg, 87.15.ap

Segregation patterns of nonequilibrium particle systems such as granulates, colloids, biopolymers, cells, and some self-propelled particles have been widely observed [1–13]. In most recent studies, the primary focus has been on the contributions of inhomogeneous particles in bulk systems.

On the other hand, in real systems, several objects are usually confined in a limited space. For example, biomolecules in cells are often confined in subcellular organelles and the reaction activities significantly differ between *in vivo* and *in vitro* situations [7,14–18]. The steady-state distribution of self-propelled particles is influenced by the characteristics of the confinement and trapping potential [19–21]. Moreover, the steady-state distributions, segregation patterns, and rheological properties of particle suspensions, binary fluids, and granular mixtures are greatly influenced by the boundary conditions such as the form and size of the container [9,11,22–26]. Thus, to uncover pattern formation mechanisms in real nonequilibrium systems, the influence of the container characteristics should be clarified.

In this study we investigate the influence of container characteristics, in particular, the container size, on the segregation patterns of two simple nonequilibrium particle models. First, we consider the segregation behavior of a hetero-Brownian particle model consisting of finite-volume particles driven by fluctuations of different magnitudes. This provides an ideal model for multicellular systems with different motilities, layers of granular particle mixtures with different friction on a horizontally vibrating bed, or mixtures of normal and laser heated hot Brownian particles [3,12,13,27]. We focus on the segregation pattern of strongly and weakly fluctuating particles where the particle motion is restricted by the combination of two familiar effects: a harmonic external trapping potential and the edge wall of a three-dimensional (3D) spherical container.

In addition, we consider a heterofluctuating polymer, which is a chain constructed by hetero-Brownian particles in a 3D spherical container without external trapping potentials. Such polymers are regarded as a simplified chromosome model for nuclei involving transcriptional active and inactive (silenced) regions [7]. Here regions containing strongly fluctuating particles are considered to be transcriptional active regions. Several proteins such as chromatin remodeling factors and transcription factors often access such active DNA regions and produce several mechanical perturbations through ATP hydrolysis energy consumption. Then, by focusing on the container-size-dependent behaviors of this model, we understand the possible contributions of biomolecule confinement in biological activities.

We now introduce the model for the hetero-Brownian particles and heterofluctuating polymer in 3D spherical containers. These systems consist of N spherical particles with diameter d. The particles are driven by random forces with different average magnitudes for each particle. The equation of motion for each particle is given by

$$\dot{\mathbf{x}}_i = -\nabla_i[V_{\rm int}(\{\mathbf{x}_i\}) + V_{\rm con}(\{\mathbf{x}_i\})] + \eta_i(t), \tag{1}$$

$$\langle \eta_i(t)\eta_i(t')\rangle = 2G_i\delta(t-t'), \tag{2}$$

where $\mathbf{x}_i$ is the position of the ith particle and η_i and G_i are the random force working on the ith particle and its magnitude, respectively. Here the origin ($\mathbf{x}_i = 0$) is the center of the container.

The interaction potential between particles is indicated by $V_{\rm int}(\{\mathbf{x}_i\})$. In the hetero-Brownian particle model, we only consider the soft-core repulsive potential as $V_{\rm int}(\{\mathbf{x}_i\}) = V^{\rm sf}(\{\mathbf{x}_i\})$ due to the excluded volumes of particles, where

$$V^{\rm sf}(\{\mathbf{x}_i\}) = \sum_{i<j} \begin{cases} \frac{k_e}{2}(|\mathbf{x}_i - \mathbf{x}_j| - d)^2 & (|\mathbf{x}_i - \mathbf{x}_j| < d) \\ 0 & (\text{otherwise}), \end{cases} \tag{3}$$

with elastic constant k_e. In the heterofluctuating polymer model, we assume that the chain of Brownian particles does not have branches. Then we have $V_{\rm int}(\{\mathbf{x}_i\}) = V^{\rm sf}(\{\mathbf{x}_i\}) + V^{\rm ch}(\{\mathbf{x}_i\})$, where

$$V^{\rm ch}(\{\mathbf{x}_i\}) = \sum_i \frac{k_c}{2}(|\mathbf{x}_i - \mathbf{x}_{i+1}| - d)^2, \tag{4}$$

with constants k_e and k_c.

The spatial constraint potential is given by $V_{\rm con}(\{\mathbf{x}_i\})$. In this study we consider $V_{\rm con}(\{\mathbf{x}_i\}) = \sum_i V^i_{\rm con}(\mathbf{x}_i)$, where $V^i_{\rm con}$ is given by the sum of potentials at the wall (edge) of the 3D spherical container $V^i_{\rm wall}$ and the external trapping potential $V^i_{\rm ex}$ as

$$V^i_{\rm wall}(\mathbf{x}_i) = \begin{cases} \frac{k_w}{2}\left[|\mathbf{x}_i| - \left(R - \frac{d}{2}\right)\right]^2 & \left(|\mathbf{x}_i| > R - \frac{d}{2}\right) \\ 0 & (\text{otherwise}) \end{cases} \quad (5)$$

and

$$V^i_{\rm ex}(\mathbf{x}_i) = \frac{k_n}{n}|\mathbf{x}_i|^n, \quad (6)$$

with constants k_w, k_n, n, and container radius R. In this study we primarily consider harmonic ($n = 2$) or linear ($n = 1$) external trapping potentials.

We now focus on the simplified systems, which contain only two types of particles: strongly fluctuating particles (S particles) with $G_i = G_s$ and weakly fluctuating particles (W particles) with $G_i = G_w$. Here we assume that G_s, k_n, and R always obey $G_s \gg k_n R^n/n$. We define the number of S and W particles as $N/2$ with $G_s = 1$, $G_w = 0$, $k_e = k_c = 1024$, and $d = 1$. When $G_w > 0$ we qualitatively obtain the same results as the $G_w \ll G_s$ case. In a heterofluctuating polymer, we also assume that the S and W particles are periodically connected where the length of each S- and W-particle region along the center of particles is $L/2$ [see Fig. 3(a)].

First, we focus on the segregation pattern formation of hetero-Brownian particles in the container with $n = 2$. When $k_2 > 0$ and $k_w = 0$, W particles (S particles) tend to locate near (far from) the container center, which may be expected by considering the G_i-dependent distribution of particles affected by the potential. On the other hand, if there exists a hard wall at the edge of the container ($k_w \gg 1$), the steady-state properties of the system change as follows.

Figures 1(a) and 1(b) show typical snapshots of the S- and W-particle distributions in the 2D cross section (particles at $-d/2 \leqslant x \leqslant d/2$ on the x-y-z 3D space are shown) for $R = 12$ and 6.5, respectively, where $k_2 = 0.001$, $k_w = 1024$, and $N = 512$. Figure 1(c) shows the relative radial distributions $P(r)$ for some R. Here $P(r) = P_W(r) - P_S(r)$, where $P_m(r) = n_m(r)/4\pi r^2$ ($m = S$ or W) are the respective radial particle distributions, r is the distance from the origin, and $n_m(r)$ is the frequency of m particles in the region between r and $r + dr$ for $dr = 0.1$. As shown in Fig. 1, the distribution of the S and W particles is greatly influenced by R: More W particles are distributed near the center than S particles for large R, while an inverted distribution occurs for small R.

The phase inversions are independent of k_2 and G_s. To understand these dependences, we study the simplest possible system with $N = 2$, which contains one S particle and one W particle. In Fig. 2(a), $\langle r\rangle = \langle r_w\rangle - \langle r_s\rangle$ are shown for several R for $k_2 = 0.01$ and 0.001, where $\langle r_w\rangle$ and $\langle r_s\rangle$ indicate the average distance of the weakly and strongly fluctuating particles from the container center, respectively. Here we obtain the value R where $\langle r\rangle = 0$, named R^*, which depends on k_2 as $R^* - d/2 \propto k_2^{-1/5}$, as shown in Fig. 2(b). Moreover, in the case of $n = 1$, we also obtain the power law where $R^* - d/2 \propto k_1^{-1/4}$ holds, as shown in Fig. 2.

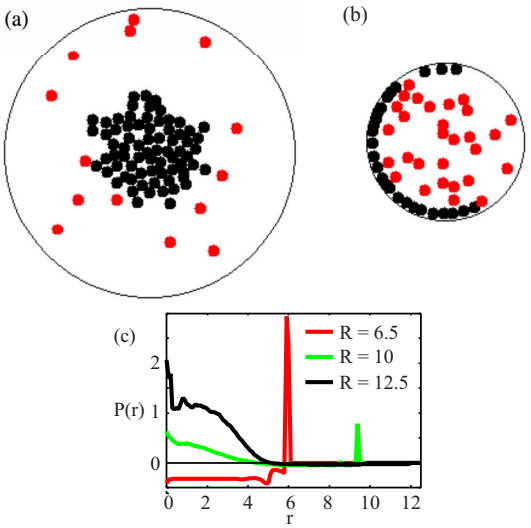

FIG. 1. (Color online) Typical snapshots of the distribution of S particles [gray (red)] and W particles (black) of the hetero-Brownian particles model ($N = 512$) on the 2D cross section for (a) $R = 12$, (b) $R = 6.5$, and (c) $P(r)$ for typical R, where r is the distance from the origin.

The mechanism of these results is considered as follows. First, we examine the case $k_n = 0$. In this case, the W-particle motion is driven only by collisions with the S particle. Once the W particle reaches the edge wall, the Sparticle tends to come from the inner region of the container. Thus, the W particles tend to stay at the edge wall independent of R.

In the cases where $k_n > 0$, the W particle tends to move toward the container center. Here the time required for the W particle to move from the edge wall to the center is estimated by $(R - d/2)/k_1$ for $n = 1$ and by $1/k_2$ for $n = 2$. On the other hand, the W particle tends to move toward the edge of the container if there are frequent collisions between S and W particles. The collision rate between S and W particles is proportional to two values: the volume fraction of the particles $[\propto (R - d/2)^{-3}]$ and the inverse of the time required for an S particle to move across the space $[\propto (R - d/2)^{-2}]$. Here G_s is assumed to be sufficiently large to make the external potential influence negligible for the S particle. Then the W particle tends to move toward the container edge if the collision rate is so large that $(R - d/2)^{-5} > \alpha k_1 (R - d/2)^{-1}$ for $n = 1$

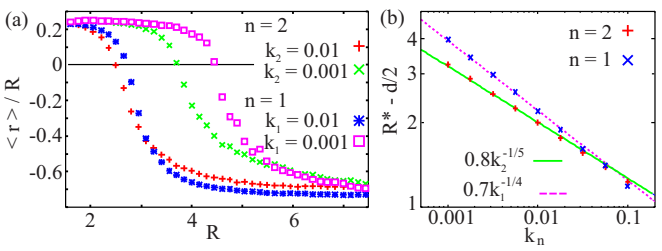

FIG. 2. (Color online) (a) Plot of $\langle r\rangle/R$ as a function of R for several k_n and (b) $R^* - d/2$ as a function of k_n for $n = 1$ and 2 in the case of $N = 2$. The solid and dashed curves in (b) are the fitted curves for each n.

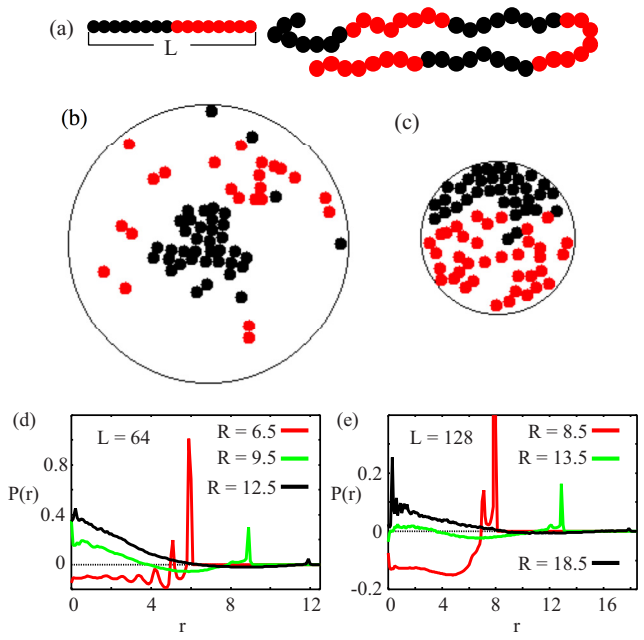

FIG. 3. (Color online) (a) Illustration of the heterofluctuating polymer model, where the black and gray (red) circles indicate weakly and strongly fluctuating particles, respectively. (b) and (c) Typical snapshots of the distributions of S particles and W particles of the heterofluctuating polymer model ($N = 512$) on the 2D cross section for $R = 11$ and 6, respectively, with $L = 64$. (d) and (e) Plots of the $P(r)$ of this model for typical R with $L = 64$ and 128, respectively.

and $(R - d/2)^{-5} > \beta k_2$ for $n = 2$ (α and β are constant values), which indicates $(R^* - d/2) \propto k_1^{-1/4}$ for $n = 1$ and $(R^* - d/2) \propto k_2^{-1/5}$ for $n = 2$.

Next we focus on the segregation of the S and W particles constructing a heterofluctuating polymer [Fig. 3(a)] in a 3D spherical container with no external trapping potentials ($k_n = 0$ and $k_w = 1024$). We focus on the cases of $L = 32$, 64, and 128 for $N = 512$. Figures 3(b) and 3(c) show typical snapshots of the particle distributions on the 2D cross section with $L = 64$ for $R = 11$ and 6, respectively, and Figs. 3(d) and 3(e) show the relative radial distribution functions of steady-state S and W particles for some R with $L = 64$ and 128, respectively. As shown in these figures, more W particles tend to be distributed at the container center than S particles for large enough R. On the other hand, W particles tend to be distributed near the edge of the container for small R.

In a recent study, only the latter segregation pattern was observed as activity-based segregation in a similar model [7]. On the other hand, our result indicates that the patterns induced by segregation generally depend on the container size [28]. We found that phase inversion occurs at $R = 9$–10 in the case of $L = 64$ and at $R = 13$–14 in the case of $L = 128$. We also found that the latter segregation pattern does not appear when $L = 32$. Therefore, these results indicate that phase inversion occurs at $R - d/2 \sim (dL/2)^{3/5}$ only if L is sufficiently large. We found similar results in the cases of $N = 256$ and 1024.

To qualitatively explain this phase inversion, we propose the following scenario. In general, the Brownian motion of a chain induces entropic force (rubber elasticity), which works on each chain element to promote chain assembly similar to the external trapping potential of the previous model. In equilibrium systems, the elasticity of the effective force is proportional to the temperature.

However, the heterofluctuating polymer consists of particles strongly and weakly fluctuating with G_s and G_w, respectively, which is equivalent to chains containing regions of high and low temperatures. Then the effective elasticity for each particle seems to be influenced by both G_s and G_w. Here it seems natural that the magnitude of the elasticity for the ith particle is proportional to G_i^*, which depends on i but always holds for $G_w < G_i^* < G_s$.

If we can neglect the effects of the excluded particle volume and the container edge, the radial distribution of each S and W particle becomes a 3D Gaussian distribution around the polymer center of mass with the variance proportional of G_s/G_i^* and G_w/G_j^*, respectively. Even when each particle has finite volume, the diversity of the S- and W-particle distribution correlates with G_s/G_i^* and G_w/G_j^*, respectively. Thus, if R is sufficiently large, more W particles are located near the polymer center of mass than S particles since $G_w/G_j^* < 1 < G_s/G_i^*$ holds for all i.

The above arguments indicate that W particles (S particles) tend to be distributed near (far from) the container center because the center of mass of the polymer tends to be close to the container center. Moreover, when R is sufficiently large, the distance between a particle at the center of S-particle region and that of the neighboring W-particle regions is estimated to be $\sim (dL/2)^{3/5}$ on average by the arguments of a self-avoiding random walk [29]. Then, if R becomes small as $R - d/2 < (dL/2)^{3/5}$, the S- and neighboring W-particle regions tend to collide excessively with each other while the force assembling the regions becomes weaker. In such cases, the W particles tend to move to the edge of the container by similar mechanisms obtained in the hetero-Brownian particle system.

If the volume fraction of the polymer is similar to that of a close-packing arrangement, we must make some corrections to the above arguments. However, the volume fractions of our simulations ($N = 256$, 512, and 1024) are considered small enough around $R - d/2 \sim (dL/2)^{3/5}$. Thus, the phase inversion R seems insensitive to N in our simulations.

In this study we investigated the segregation patterns of strongly and weakly fluctuating Brownian particles confined in a spherical container. We found that the segregation patterns of such systems depend on the container size. Our present results provide a significant contribution to our understanding of the formation mechanism and selection of segregation patterns for several real nonequilibrium particle populations. In particular, the heterofluctuating polymer model plays an important role in the clarification of chromosome behaviors in the cell nucleus.

In particular, the cell nucleus size changes at different cell cycles and the cell types differ throughout multicellular-organism development even though the volume and length of the chromosome in each cell remain the same [30–34]. The distribution of transcriptional active and inactive DNA regions caused by DNA methylations and heterochromatin formations also depends on the conditions of the cells [33–35]. The difference in cell conditions greatly influences the chromosome dynamics that contribute to specific gene

regulations of each cell type and cell cycle. For example, variation in the sequential position of the methylated sequences and the heterochromatins contributes to drastic changes of the spatial positioning of heterochromatins [33–35].

The container-size-dependent (nucleus-size-dependent) pattern formations and the pattern formations caused by periods of strong and weak fluctuations along the polymer (transcriptional active and inactive regions along the DNA sequence) provide several insights into the above experimental conditions. We also note that the elasticity and heterogeneity of the chain play important roles in the pattern formation [6,36].

The author is grateful to T. Sugawara, S. Shinkai, S. Lee, T. Sakaue, and H. Nishimori for fruitful discussions. This research was supported in part by the Platform for Dynamic Approaches to Living System from the Ministry of Education, Culture, Sports, Science and Technology, Japan, and the Grant-in-Aid for Scientific Research on Innovative Areas "Spying minority in biological phenomena" (Grants No. 3306 and No. 24115515) and "Initiative for High-Dimensional Data-Driven Science through Deepening of Sparse Modeling" (Grants No. 4503 and No. 26120525) of MEXT of Japan.

[1] P. L. Townes and J. Holtfreter, J. Exp. Zool. **128**, 53 (1955).
[2] M. S. Steinberg, Curr. Opin. Gen. Dev. **17**, 281 (2007).
[3] R. M. H. Merks and J. A. Glazier, Physica A **352**, 113 (2005).
[4] S. R. McCandlish, A. Baskaran, and M. F. Hagan, Soft Matter **8**, 2527 (2012).
[5] Y. Fily and M. C. Marchetti, Phys. Rev. Lett. **108**, 235702 (2012).
[6] K. Finan, P. R. Cook, and D. Marenduzzo, Chromosome Res. **19**, 53 (2011).
[7] N. Ganai, S. Sengupta, and G. I. Menon, Nucleic Acids Res. **42**, 4145 (2014).
[8] A. Wysocki and H. Löwen, Phys. Rev. E **79**, 041408 (2009).
[9] J. B. Knight, H. M. Jaeger, and S. R. Nagel, Phys. Rev. Lett. **70**, 3728 (1993).
[10] A. Awazu, Phys. Rev. Lett. **84**, 4585 (2000).
[11] A. Awazu, J. Phys. Soc. Jpn. **72**, 1832 (2003).
[12] T. Mullin, Phys. Rev. Lett. **84**, 4741 (2000).
[13] M. Fujii, A. Awazu, and H. Nishimori, Phys. Rev. E **85**, 041304 (2012).
[14] F. Takagi, N. Koga, and S. Takada, Proc. Natl. Acad. Sci. U.S.A. **100**, 11367 (2003).
[15] D. Kilburn, J. H. Roh, L. Guo, R. M. Briber, and S. A. Woodson, J. Am. Chem. Soc. **132**, 8690 (2010).
[16] J. Lin, A. Harding, E. Giurisato, and A. S. Shaw, Mol. Cell. Biol. **29**, 2082 (2009).
[17] K. Aoki, M. Yamada, K. Kunida, S. Yasuda, and M. Matsuda, Proc. Natl. Acad. Sci. U.S.A. **108**, 12675 (2011).
[18] M. Fujii, H. Nishimori, and A. Awazu, PLoS ONE **8**, e62218 (2013).
[19] H. H. Wensink and H. Löwen, Phys. Rev. E **78**, 031409 (2008).
[20] R. W. Nash, R. Adhikari, J. Tailleur, and M. E. Cates, Phys. Rev. Lett. **104**, 258101 (2010).
[21] C. F. Lee, New J. Phys. **15**, 055007 (2013).
[22] C. Bechinger, Curr. Opin. Colloid Interface Sci. **7**, 204 (2002).
[23] M. E. Cates, R. Adhikari, and K. Stratford, J. Phys.: Condens. Matter **17**, S2771 (2005).
[24] C. Lundell, E. H. A. de Hoog, R. H. Tromp, and A.-M. Hermansson, J. Colloid Interface Sci. **288**, 222 (2005).
[25] R. Verberg, C. M. Pooley, J. M. Yeomans, and A. C. Balazs, Phys. Rev. Lett. **93**, 184501 (2004).
[26] M. E. Cates, S. M. Fielding, D. Marenduzzo, E. Orlandini, and J. M. Yeomans, Phys. Rev. Lett. **101**, 068102 (2008).
[27] D. Rings, R. Schachoff, M. Seimke, F. Cichos, and K. Kroy, Phys. Rev. Lett. **105**, 090604 (2010).
[28] Reference [7] also reported a similar phase inversion by assuming anomalous boundary conditions. However, no experimental evidence for this assumption exists at this time.
[29] P.-G. de Gennes, *Scaling Concepts in Polymer Physics* (Cornell University Press, London, 1979).
[30] J. Newport and M. Kirschner, Cell **30**, 675 (1982).
[31] P. Jorgensen, N. P. Edgington, B. L. Schneider, I. Rupeš, M. Tyers, and B. Futcher, Mol. Biol. Cell **18**, 3523 (2007).
[32] F. R. Neumann and P. Nurse, J. Cell Biol. **179**, 593 (2007).
[33] I. Solovei, M. Kreysing, C. Lanctôt, S. Kösem, L. Peichl, T. Cremer, J. Guck, and B. Joffe, Cell **137**, 356 (2009).
[34] I. Solovei *et al.*, Cell **152**, 584 (2013).
[35] S. Kobayakawa, K. Miike, M. Nakao, and K. Abe, Genes Cell **12**, 447 (2007).
[36] N. Stoop, J. Najafi. F. K. Wittel, M. Habibi, and H. J. Herrmann, Phys. Rev. Lett. **106**, 214102 (2011).